Purification of Curcumin from Ternary Extract-Similar Mixtures of Curcuminoids in a Single Crystallization Step

Elena Horosanskaia [1], Lina Yuan [1], Andreas Seidel-Morgenstern [1,2] and Heike Lorenz [1,*]

[1] Max Planck Institute for Dynamics of Complex Technical Systems, Sandtorstrasse 1, 39106 Magdeburg, Germany; horosanskaia@mpi-magdeburg.mpg.de (E.H.); lina.yuan@novartis.com (L.Y.); anseidel@ovgu.de (A.S.-M.)

[2] Otto von Guericke University, Institute of Process Engineering, Universitätsplatz 2, 39106 Magdeburg, Germany

[*] Correspondence: lorenz@mpi-magdeburg.mpg.de

Abstract: Crystallization-based separation of curcumin from ternary mixtures of curcuminoids having compositions comparable to commercial extracts was studied experimentally. Based on solubility and supersolubility data of both, pure curcumin and curcumin in presence of the two major impurities demethoxycurcumin (DMC) and bis(demethoxy)curcumin (BDMC), seeded cooling crystallization procedures were derived using acetone, acetonitrile and 50/50 (wt/wt) mixtures of acetone/2-propanol and acetone/acetonitrile as solvents. Starting from initial curcumin contents of 67–75% in the curcuminoid mixtures single step crystallization processes provided crystalline curcumin free of BDMC at residual DMC contents of 0.6–9.9%. Curcumin at highest purity of 99.4% was obtained from a 50/50 (wt/wt) acetone/2-propanol solution in a single crystallization step. It is demonstrated that the total product yield can be significantly enhanced via addition of water, 2-propanol and acetonitrile as anti-solvents at the end of a cooling crystallization process.

Keywords: curcumin; purification; ternary mixture of curcuminoids; crystallization

1. Introduction

Curcumin (abbreviated CUR), known as diferuloyl methane, is an intense orange-yellow solid and a natural ingredient of the plant rhizome of *Curcuma Longa* L. Two derivatives of CUR, demethoxycurcumin (abbreviated DMC) and bis(demethoxy)curcumin (abbreviated BDMC), can be found in the plant as well. Altogether they are known as curcuminoids (abbreviated CURD). Depending on the soil condition, the total content of CURDs in the plant rhizome varies between 2 and 9%. With approximately 70% of the total CURD content CUR represents the major component in turmeric [1–3]. As highlighted in Figure 1, the presence or absence of a methoxy functional group on o-position to a phenolic group represents the only difference in the chemical structure of the three CURDs. The molecular structure of CUR comprising two equally substituted aromatic rings linked together by a diketo group, which exhibits keto-enol tautomerism, plays a crucial role in the reactivity of CUR [4,5].
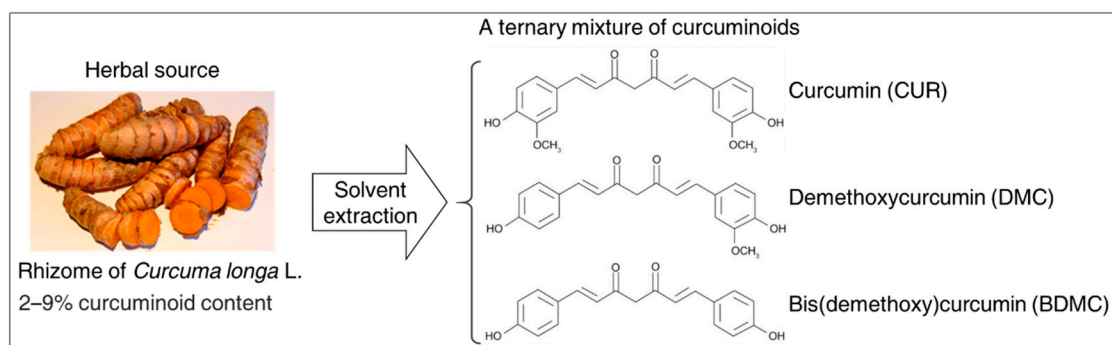
Figure 1. Curcuminoids extracted from the rhizome of Turmeric (*Curcuma longa* L.) and molecular structures of the three major constituents (curcumin (CUR), demethoxycurcumin (DMC) and bis(demethoxy)curcumin (BDMC)).

Studies show that CUR can be potentially used to treat over 25 diseases due to its anti-oxidative, immunosuppressive, wound-healing, anti-inflammatory and phototoxic effects [6–8]. These include, in particular, neurodegenerative diseases, such as Alzheimer's and Parkinson's diseases, diabetes, heart sickness, bacterial, viral and fungal diseases, AIDS and over 20 different cancers [9–12]. In addition to CUR, also the potential use of DMC and BDMC in the prevention of cancer was emphasized [13–15]. It was reported that DMC has the stronger effect on the inhibition of human breast tumor cells, followed by CUR and BDMC [16]. Ruby et al. described the higher bioavailability and cytotoxic activity of BDMC in animal cells [17].

Due to the higher reactivity of CUR associated with the stronger pharmacological activity on the human body comparable to the two other derivatives, CUR currently remains the targeted turmeric compound [18]. Despite the diverse pharmacological effects, the practical insolubility of CUR in water results in a very low bioavailability of the molecule and therewith leads to a limited usage as a drug [19]. To improve the bioavailability, formulation of curcumin nanoparticles or metal complexes were successfully implemented [20,21]. In addition, the application of CUR together with artemisinin in a CUR-artemisinin combination therapy against malaria was reported to decrease the drug resistance [22]. Moreover, the formulation of a CUR-artemisinin co-amorphous solid showed a higher therapeutic effect in the treatment of cancer than the single drug formulation [23]. For each of the application, CUR has to be available in chemically pure form and in sufficient amount.

H.J.J. Pabon described the preparation of synthetic CUR and related compounds [24]. Kim et al. recently published a process for production of CURDs in engineered Escherichia coli [25]. Nevertheless, the separation of CUR by means of solvent extraction from the plant rhizome still represents the most economical way of CUR production. In addition to plant proteins, oils and fats, the final extract contains 80% of the ternary CURD mixture [26]. In this mixture CUR is the major component with approximately 64% share of the total CURD content, together with 21% DMC and 15% BDMC [27]. Commercially available mixture usually contains 77% CUR, 17% DMC and 6% BDMC [28]. Consequently, CUR has to be purified from the ternary mixture.

There are two methods for separation of CUR from the mixture of CURDs described in the literature: by means of column or thin layer chromatography and by crystallization from solution.

For the chromatographic separation of CUR, silica gel (untreated or impregnated with sodium hydrogen phosphate) is commonly used as a stationary phase and various binary solvent mixtures of dichloromethane, chloroform, methanol, acetic acid, ethyl acetate and hexane as the mobile phase [29]. At the end of the process, three chromatographic fractions are enriched with the three CURDs, respectively [30,31]. Usually crystallization is applied as the final formulation step providing the solid product with desired specifications.

In the last decade, crystallization as a single separation technique was studied to purify CUR from the ternary mixture of curcuminoids [32–34]. Processes were described exploiting anti-solvent

addition or system cooling, using methanol, ethanol and 2-propanol as process solvents and water as anti-solvent (Table 1).

Table 1. Overview of the results of published studies on CUR purification via crystallization: References 1–3 relate to [32–34], respectively.

Reference	Raw Mixture Content of CUR %	DMC %	Solvent	Crystallization Method	No. of Crystallization Steps	Product Content of CUR %	DMC %	Total Yield %
1	/[1]	/[1]	Methanol	Anti-solvent addition, water	3	92.2	7.8	40
2	82.0	16.0	Ethanol	Cooling, 70 °C to 5 °C	2	96.0	4.0	/[1]
3	78.6	17.7	2-Propanol	Cooling, 60 °C to 20 °C	3	>98/99.1[2]	<2/0.9[2]	50[2]

[1] not specified; [2] optimized crystallization conditions.

As summarized in Table 1, from initial CURD mixtures crystalline CUR with purities of 92.2%, 96.0% and 99.1% at overall yields between 40 and 50% were obtained. The used separation methods were implemented as multi-step processes consisting of at least two successive sub-steps. It is reported that the main part of BDMC could be depleted after the first separation step, full removal was achieved after the second crystallization step [33,34]. DMC was always present in the final product. Ukrainczyk et al. observed an exponential decrease of the removal efficiency of DMC with increasing number of successive crystallization steps [34].

In order to reach the desired product purity and also to improve the overall process yield, a combination of the two separation techniques, chromatography and crystallization, was recently studied. Horvath et al. successfully implemented this integrated process for recovery of 99.1% pure artemisinin from an effluent of a photocatalytic reactor with 61.5% yield [35]. Heffernan et al. demonstrated the purification of single CURDs from the crude curcumin extract. There, the firstly performed crystallization process comprised three crystallization cycles, which provided 99.1% pure CUR in the final crystalline product. In the second process step, the remaining mother liquor was processed by column chromatography to isolate DMC and BDMC with purities of 98.3% and 98.6% and yields of 79.7% and 68.8%, respectively [36].

As has been demonstrated for other natural product mixtures, crystallization is a powerful technique to isolate a target compound from a multicomponent mixture within a single crystallization step [37,38]. Due to the fact that a 98% minimum purity of CUR is already sufficient for further drug application in pharmaceutical preparations [22], this study is directed to develop a separation process for isolation of pure crystalline CUR from the ternary mixture of CURDs within a single crystallization step.

To separate a target compound from a multi-component mixture, seeded cooling crystallization is preferably applied. Anti-solvent is usually added either at the beginning of the cooling step to generate the supersaturation in the solution or at the end of the process to increase the overall crystallization yield [39].

To purify CUR from the crude CURD mixture, seeded cooling crystallization processes were designed on the basis of solubility and nucleation measurements of pure CUR and CUR in presence of the CURDs mixture components in acetone, acetonitrile, ethanol, methanol, 2-propanol and selected binary mixtures thereof. Finally, with respect to the solubility results, 2-propanol, acetonitrile and water were considered as anti-solvents to improve the overall process yield.

2. Materials and Methods

2.1. Materials

Solid standards of curcumin, demethoxycurcumin (both >98%, TCI Chemicals) and bis(demethoxy)curcumin (>99%, ChemFaces China) were used as standards for HPLC and X-ray powder diffraction (XRPD) analysis. The solid standard of curcumin was also used to determine the solubility and nucleation behaviors. During the study, four crude solid mixtures of CURDs were purchased from Sigma Aldrich and Acros. The content of CUR, DMC and BDMC in the solids, determined by means of HPLC, is summarized in Table 2.

Table 2. Comparison of the crude solids purchased from Sigma Aldrich (crude solids No. 1–3) and Acros (crude solid no. 4), each representing a ternary mixture of the three CURDs.

Crude Solid No.	CUR Content wt%	DMC Content wt%	BDMC Content wt%
1	67.2	25.5	7.3
2	70.8	23.5	5.7
3	75.0	19.2	5.8
4	80.7	16.5	2.8

The highest CUR content of 80.7% was found in the crude solid obtained from Acros. The CUR content in the crude solids from Sigma Aldrich varies between 67.2% and 75.0% depending on the purchased charge, but is most similar to that of plant extract [28]. Accordingly, the solids from Sigma Aldrich were used as crude mixture for crystallization experiments. It should be emphasized that the analyzed significant differences of the CUR content in the three solid charges made the implementation of the designed crystallization process more challenging.

Acetone, acetonitrile, ethanol, methanol and 2-propanol (>99.8%, HiPerSolv CHROMANORM, VWR Chemicals, Germany) were used for solubility studies and for the crystallization experiments.

2.2. Analytical Methods

An analytical HPLC unit (Agilent 1200 Series, Agilent Technologies Germany GmbH) was used to characterize the solid standards, to quantify the CUR, DMC and BDMC contents in the crude mixtures as well as in the final crystallization products. The reversed phase method reported by Jadhav et al. [40] was adjusted as follows: the mobile phase composition was fixed to 50/50 (vol/vol) acetonitrile/0.1% acetic acid in water. Before usage water was purified via Milli-Q Advantage devices (Merck Millipore). The eluent flow-rate was set to 1 mL/min. Solid samples preliminarily dissolved in acetonitrile were injected (injection volume 1 µL) in the column (LUNA C18, 250 × 4.6 mm, 10 µm, Phenomenex GmbH, Germany, column temperature 25 °C) and analyzed at a wavelength of 254 nm. Figure 2 shows chromatograms of the solid standards of BDMC, DMC and CUR compared to a ternary mixture of CURDs (exemplarily crude solid No. 3).

X-ray powder diffraction (XRPD) was applied to characterize the purchased solid standards, solid fractions obtained during the solubility studies and the crystallization products. For the measurements, solid samples were ground in a mortar and prepared on background-free Si single crystal sample holders. Data were collected on an X'Pert Pro diffractometer (PANalytical GmbH, Germany) using Cu-Kα radiation. Samples were scanned in a 2Theta range of 4 to 30° with a step size of 0.017° and a counting time of 50 s per step.

2.3. Solubility and Metastable Zone Width Measurements

Solubility investigations of pure CUR in acetone, acetonitrile, ethanol, methanol and 2-propanol were carried out via the classical isothermal method [41]. To evaluate the impact of the main impurities (DMC and BDMC) on the solubility behavior of CUR, the crude mixture of CURDs no. 2 was used in selected process solvents. Suspensions containing excess of solid CUR and 5 mL solvent were

introduced in glass vials. To guarantee efficient mixing of the prepared suspensions, vials were equipped with a magnetic stirrer and sealed. Samples were placed in a thermostatic bath and allowed to equilibrate at constant temperatures between 5 and 70 °C for at least 48 h under stirring. Afterwards, samples of equilibrated slurries were withdrawn with a syringe and filtered through a 0.45 μm PTFE filter. Obtained liquid phases were analyzed for solute content by HPLC. To preserve equilibrium conditions for low temperature samples, syringes and filters were precooled before usage. The corresponding wet solid fractions were characterized by XRPD.
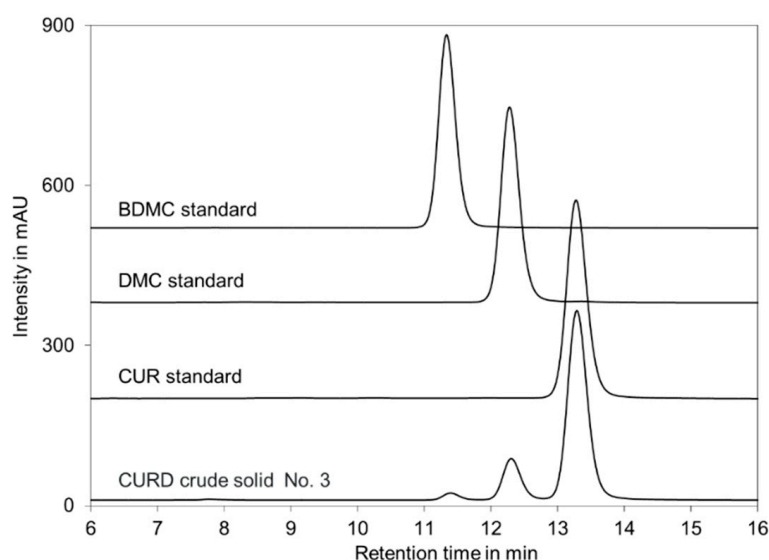

Figure 2. Analytical HPLC chromatograms of solid standards of BDMC, DMC, CUR and of the crude mixture No. 3 (see Table 1).

Metastable zone width data of pure CUR in selected process solvents were acquired by means of the multiple reactor system Crystal16^{TM} (Avantium Technologies BV, Amsterdam). Suspensions containing known excess amount of solid in solvent were prepared in standard HPLC glass vials, equipped with magnetic stirrers and subjected to a heating step from 5 to 60 °C and a subsequent cooling step from 60 to −15 °C, both at a moderate rate of 0.1 °C/min. Temperatures of a "clear" and "cloud" point representing the respective saturation and nucleation temperatures were obtained via turbidity measurement.

Batch crystallization experiments were conducted in a jacketed 200 mL glass vessel equipped with a Pt-100 resistance thermometer (resolution 0.01 °C) connected to a thermostat (RP845, Lauda Proline, Germany) to control the system temperature. A magnetic stirrer was used for agitation.

With respect to the determined solubility behavior of CUR, four process solvents were selected. Consequently, four cooling crystallization processes were derived and conducted. Table 3 gives an overview of the chosen process solvents and the CURD mixtures to be separated. Exact solution composition data (Table 5) and the applied crystallization procedures are presented and discussed in connection with crystallization process design in Sections 3.2 and 3.3.

Table 3. Overview of the selected process solvents and the corresponding crude solids.

Process No.	Process Solvent	Crude Solid No.
1	Acetone	3
2	50/50 (wt/wt) acetone/2-propanol	2
3	50/50 (wt/wt) acetone/acetonitrile	1
4	Acetonitrile	1

3. Results and Discussion

3.1. Selection of Solvents for Crystallization

To design a crystallization-based purification process, the selection of an appropriate solvent is crucial. The operation parameters for the crystallization process are established based on the specific solubility and nucleation behavior of the target compound in the corresponding solvent.

3.1.1. CUR Solubility in Acetone, Acetonitrile, Methanol, Ethanol and 2-propanol

Acetone, acetonitrile, methanol, ethanol and 2-propanol were selected as possible process solvents because of their low toxicity. CUR solubilities determined in these solvents are shown in Figure 3. As seen CUR solubilities increase with increasing temperature in all solvents. Compared to acetone, CUR is significantly less soluble in the other solvents (less than 1 wt%, except in acetonitrile at 40 °C). Hence, acetone was chosen as a suitable solvent for seeded cooling crystallization and acetonitrile, methanol, ethanol and 2-propanol were considered as potential anti-solvents. According to the published very poor solubility of CUR in water (approx. 1.3×10^{-7} wt% at 25 °C) water was also taken into account as anti-solvent without extra solubility studies [20].
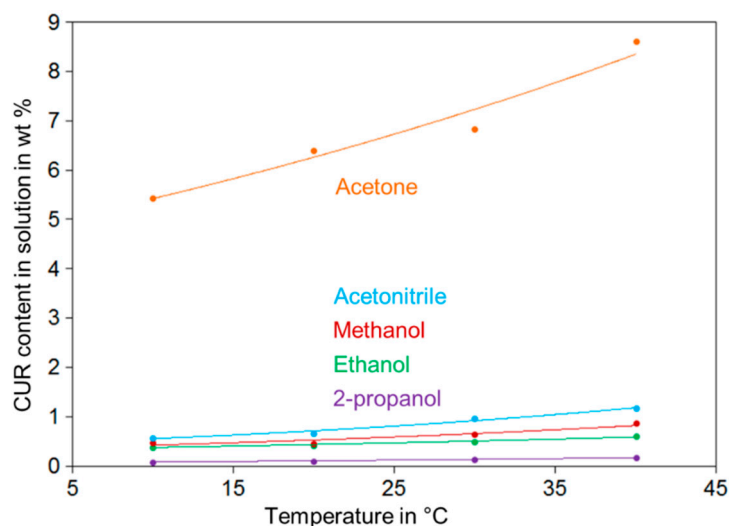

Figure 3. Solubility behavior of CUR in acetone, acetonitrile, methanol, ethanol and 2-propanol. Symbols represent experimental data, fitted curves just serve as guide to the eyes.

In Figure 4, CUR solid phase XRPD patterns are shown obtained from isothermal equilibration of CUR suspensions (Figure 4a), and by (polythermal) cooling of saturated CUR/solvent mixtures (Figure 4b–f). Measured patterns are compared with references for the three CUR polymorphs derived from single crystal data given in the Cambridge Structural Database (CSD) [42].

Commercial solid standard of CUR, which represents the initial solid for isothermal solubility studies, and all CUR solid phases obtained in equilibrium with saturated solutions in the solvents studied (Figure 4a) perfectly match the pattern of the known CUR polymorph I. XRPD patterns obtained for CUR recrystallized polythermally from acetone and acetonitrile solutions (Figure 4b,c) can be assigned to CUR I as well. CUR phases obtained by cooling of saturated methanol, ethanol and 2-propanol solutions (Figure 4d–f) do not match any shown reference phase, but (except a small missing reflex at 6.8° in the ethanol pattern) are identical to each other. Aside from that, their XRPD patterns differ from the CUR I phase only by some additional reflexes in the 2Theta range of 6°–8°. One hypothesis explaining this behavior might be incorporation of small amounts of respective alcohol molecules in the crystal structure without changing the structure type. Further, according to the known complex solid phase behavior of CUR [42–48] and BDMC [49,50], also the formation of a new

metastable form of CUR in the three alcohols or a solvate phase from ethanol are possible explanations. Since elucidation of the CUR phase behavior was not the main focus of the present study, this issue has to be verified in future investigations.
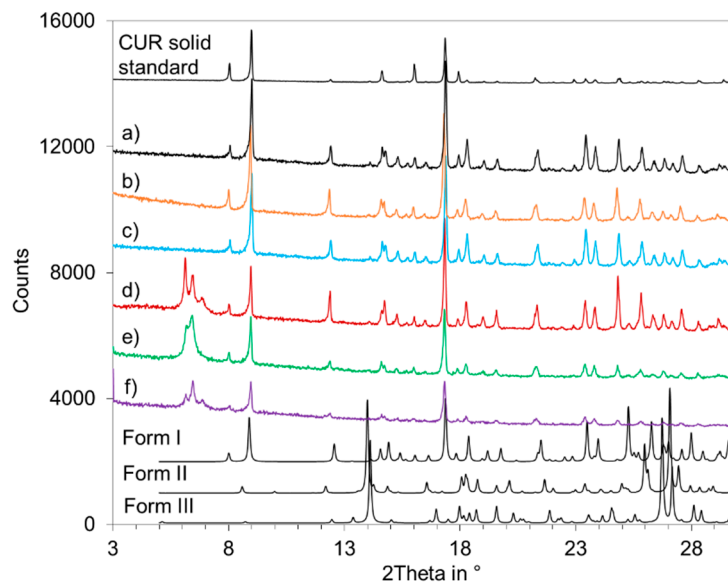

Figure 4. X-ray powder diffraction (XRPD) patterns of CUR crystalline phases (**a**) obtained from isothermal equilibration of CUR suspensions, and (**b–f**) recrystallized by cooling of saturated CUR solutions in acetone (**b**), acetonitrile (**c**), methanol (**d**), ethanol (**e**), 2-propanol (**f**). The topmost diffractogram refers to the CUR solid standard. The three lowermost diffractograms specify the reference crystal structures of CUR polymorphs I-III simulated from CSD single crystal data [42].

With the aim to selectively crystallize pure CUR (form I) from the crude CURD solution and to suppress spontaneous nucleation of undesired DMC and BDMC components, seeding with CUR solid standard (form I) was applied in cooling crystallization experiments.

To evaluate the anti-solvents effect on the CUR solubility in acetone, saturation concentrations of CUR (solid standard) were measured at 30 °C in the 50/50 (wt/wt) acetone/anti-solvent mixtures, exemplarily. Figure 5 shows that the obtained solubility data of CUR in the four binary solvent mixtures deviate from the ideal linear behaviors. Moreover, it is seen that the addition of methanol, ethanol and 2-propanol induces a dilution effect rather than the expected supersaturation of the solution. Since the relative dilution effect of ethanol and methanol is larger than that of 2-propanol, they are not considered further for crystallization process design. In contrast, the addition of acetonitrile increases the supersaturation of CUR in acetone. Therefore, a high product yield can be expected. Consequently, the following four process solvents were selected to conduct the seeded cooling crystallization of CUR: pure acetone and acetonitrile as well as 50/50 (wt/wt) mixtures of acetone/2-propanol and acetone/acetonitrile.

3.1.2. Effect of DMC and BDMC on CUR Solubility in the Selected Process Solvents

Before designing seeded cooling crystallizations, the solubility behavior of CUR was evaluated in presence of the main impurities DMC and BDMC in acetone, 50/50 acetone/2-propanol, 50/50 acetone/acetonitrile and acetonitrile. In Figure 6, the resulting solubility data are compared with the solubility values of pure CUR in the respective solvents.
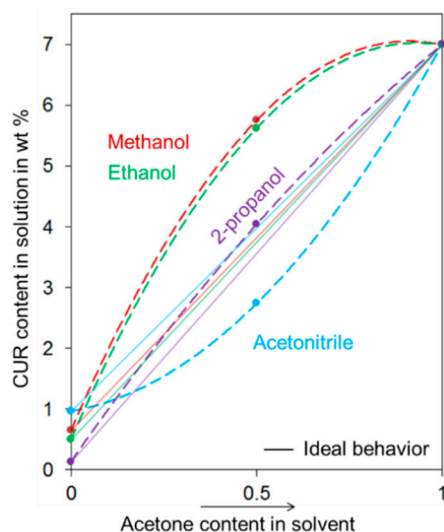
Figure 5. Effect of anti-solvents methanol, ethanol, 2-propanol and acetonitrile on the solubility of CUR in acetone at 30 °C. Symbols represent experimental data, curves are just guide to the eyes. Dashed curves originate from experimentally determined solubility values in the respective 50/50 (wt/wt) acetone/anti-solvent mixtures. Thin solid lines represent ideal linear solubility behaviors.
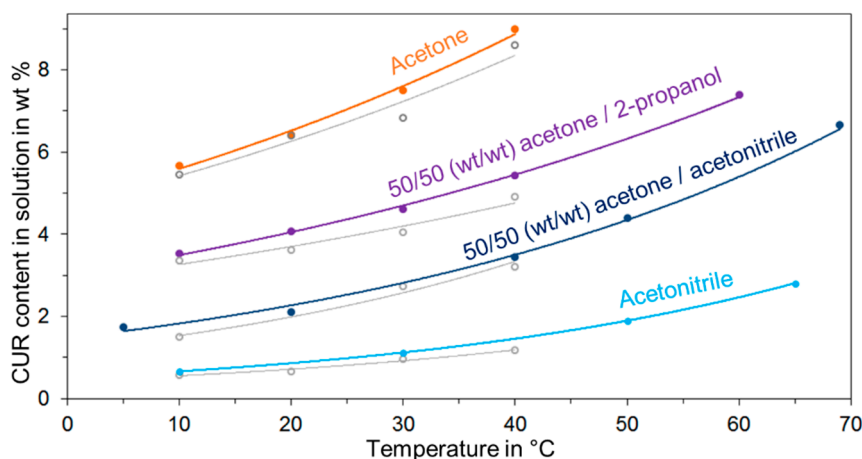

Figure 6. Comparison of solubility curves determined for pure CUR (empty circles, grey curves), and CUR in presence of the main impurities (solid circles, colored curves). Symbols represent experimental data, fitted curves serve as guide to the eyes.

As seen the solubilities of CUR in presence of DMC and BDMC slightly exceed those of pure CUR in the four solvents. Moreover, comparison of the CUR solubility in 50/50 acetone/2-propanol and 50/50 acetone/acetonitrile shows that with the use of acetonitrile as anti-solvent, a higher supersaturation of CUR in the solution can be obtained resulting in a higher product yield. This observation confirms the behavior of pure CUR in the binary solvents discussed in Figure 5.

3.2. Design of the Seeded Cooling Crystallization for Separation of CUR

Based on the solubility curves of CUR in presence of the main impurities and the observed nucleation behavior of pure CUR in the respective solvents, four seeded cooling crystallization processes were derived to separate CUR from the CURD mixtures as illustrated in Figure 7.
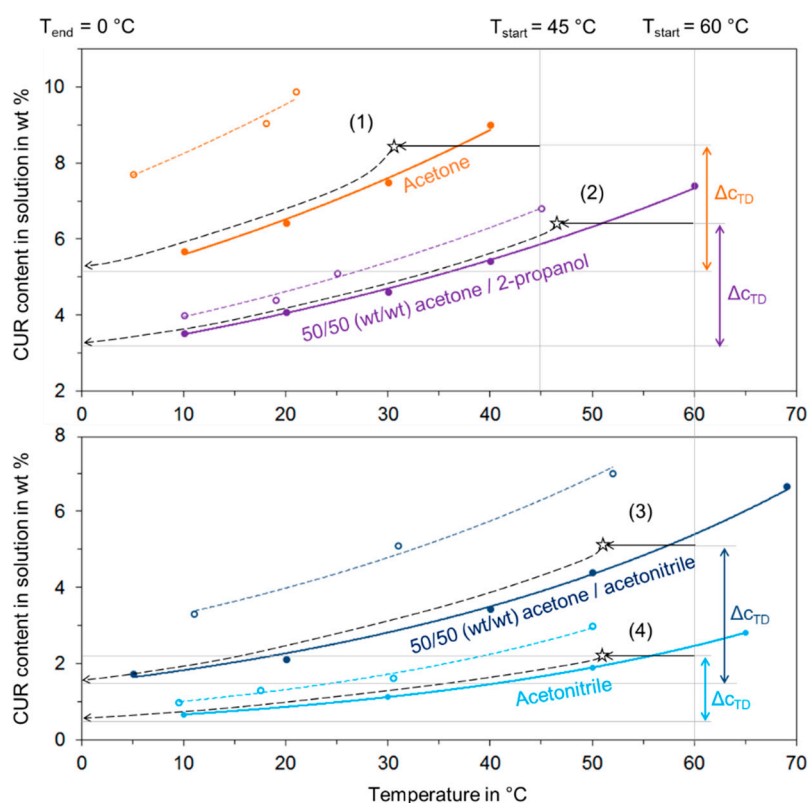
Figure 7. Design of the seeded cooling crystallization processes of CUR based on the solubility curves of CUR in presence of the main impurities (solid lines) and the nucleation border of pure CUR (dashed lines) in acetone (1), 50/50 acetone/2-propanol (2), 50/50 acetone/acetonitrile (3) and acetonitrile (4). Black solid/dashed lines with arrows are imaginary curves representing the variation of the CUR concentration during the crystallization process. (T_{start}/T_{end}: start/end temperature of the cooling step; stars: temperature of seed addition; Δc_{TD}: maximal depletion of CUR from solution).

The starting temperatures of the crystallization processes in the 50/50 mixtures of acetone/2-propanol and acetone/acetonitrile and in acetonitrile were set at 60 °C. To avoid uncontrolled evaporation of acetone, 45 °C was chosen as the starting temperature in this solvent.

The temperatures at which seeds of pure CUR (form I) were introduced into the acetone, 50/50 acetone/acetonitrile and acetonitrile solutions were chosen to be at least 5 K below the saturation temperature of CUR (approximately in the first third of the metastable region). However, the metastable region of CUR in 50/50 acetone/2-propanol (Figure 7, purple lines) is significantly closer than for the other three solvent systems. Therefore, the seeds were added at approximately half of the metastable region. An overview of the selected process parameters for the four seeded cooling crystallization processes is given in Table 4.

Table 4. Overview of the selected crystallization process parameters.

Process No.	Process Solvent	T_{start} °C	T_{sat} °C	T_{seeds} °C	T_{end} °C	Cooling Rate K/h
1	Acetone	45	37	30	0	10
2	50/50 acetone/2-propanol	60	51	46	0	10
3	50/50 acetone/acetonitrile	60	57	51	0	10
4	Acetonitrile	60	56	51	0	10

T_{start}/T_{end}: start/end temperature of cooling step; T_{sat}: CUR saturation temperature; T_{seeds}: seeding temperature.

The initial concentrations of CUR in the crude CURD mixtures were selected in accordance with the set starting temperatures to guarantee undersaturation of CUR in the starting solutions. The amounts of the crude solids, the process solvents and the calculated initial CUR content in the four starting solutions are listed in Table 5.

Table 5. Amount of initial substances used in the four crystallization processes.

Process No.	m (CURD) g	m (Solvent) g	c_{start} (CUR) wt%	$c_{end} = c_{sat}$ (CUR) wt%	Δc_{TD} (CUR) wt%	m_{max} (CUR) g
1	19.0	150	8.4	5.1	3.3	5.7
2	14.0	150	6.4	3.2	3.2	5.1
3	11.5	140	5.1	1.5	3.6	5.5
4	5.2	150	2.2	0.5	1.7	2.7

m(CURD), m(Solvent): amounts of CURD mixture and solvent used for the starting solution; c_{start}(CUR): calculated concentration of CUR in the starting solution; $c_{end}=c_{sat}$: concentration of CUR at the end of the cooling process, equal to the respective saturation concentration, from solubility study; Δc_{TD}(CUR): max. possible change of CUR concentration at the end of the cooling process, calculated based on the thermodynamic values; m_{max}: maximal achievable mass of CUR, calculated based on the thermodynamic values.

3.3. Implementation of the Purification Process

In the first step, the four initial crude solutions were prepared using the corresponding amount of the crude solid mixture in the respective solvent (Table 5). The seeded cooling crystallization of CUR was conducted in a second step following the four process trends shown in Figure 7. Starting at set temperatures, the unsaturated clear solutions were cooled down to 0 °C at a linear rate of 10 K/h. After exceeding the corresponding saturation temperature, seed crystals of pure CUR form I (ca. 50 mg) were introduced into the supersaturated solution at T_{seeds} (Table 4). At the end of the cooling process at 0 °C, the obtained product suspensions were stirred for further 0.5 h. Subsequently, solid-liquid phase separation was carried out on suction filters (pore size of filter paper 0.6 μm). To remove adhering mother liquor from the filter cake, the collected crystals were washed with about 100 g of cold acetone (< 0 °C, in processes 1-3) or with acetonitrile (< 0 °C in process 4). Then, dried at 40 °C, the purity of CUR and the yield were analyzed. During the washing process with acetone a visible dissolution of the filter cake was observed, caused by the high solubility of CUR in acetone (about 5 wt% at 0 °C). Accordingly, lower product yields could be assumed in the processes of using acetone as washing solvent (in processes 1-3).

The results of the four conducted seeded cooling crystallizations are summarized in Table 6. The maximum thermodynamically possible yield of CUR η_{TD} was calculated according to Equation (1), the total product yield of CUR η according to Equation (2).

$$\eta_{TD}(CUR) = \frac{m_{product} \cdot CUR\ product\ content}{m_{max}} \tag{1}$$

$$\eta(CUR) = \frac{m_{product} \cdot CUR\ product\ content}{m_{start}(CUR)} \tag{2}$$

Table 6 shows that in the 50/50 acetone/2-propanol mixture (process 2), the highest purity of CUR (99.4%) in the crystalline product was achieved. However, only 13% of the initial CUR content in the crude mixture was recovered. Crystalline CUR with decreasing purity of 95.7%, 92.3% and 90.1% but increasing total product yields of 31%, 55% and 62% was obtained from acetone, acetonitrile and 50/50 acetone/acetonitrile, respectively. The lower total yields from acetone and acetone/2-propanol solutions are partly associated with the enhanced CUR solubility at the final process temperature compared to the acetonitrile-containing solutions (see Figure 7), which, however, does not explain the extremely low yield achieved in the latter case.

The obtained purity results further verify that BDMC could completely be removed from the crystalline products within a single separation step, while the content of DMC was noticeably reduced. The presence of DMC as impurity in the products can be probably attributed to the most similar

molecular structure of DMC and CUR (Figure 1). It can be postulated that DMC molecules compete with CUR in the solution upon forming the main crystal lattices. To ascertain, whether DMC is present near CUR in the crystalline form or as amorphous phase, the four crystallization products were analyzed by XRPD. In Figure 8 the corresponding patterns are compared with the commercial solid standards of DMC and CUR.

Table 6. Results of the four seeded cooling crystallization processes. Table columns containing the products purity and yield are highlighted in grey.

Process No.		Ternary Mixture of Curcuminoids					Crystalline Product					
	Process Solvent	m_{start} (CUR)	CUR Content	DMC Content	BDMC Content	m_{max} (CUR)	m (Product)	CUR Content	DMC Content	BDMC Content	η_{TD} (CUR)	η (CUR)
		g	%	%	%	g	g	%	%	%	%	%
1	Acetone	14.3	75.0	19.2	5.8	5.7	4.6	95.7	4.3	0	77	31
2	50/50 acetone/ 2-propanol	9.9	70.8	23.5	5.7	5.1	1.3	99.4	0.6	0	25	13
3	50/50 acetone/ acetonitrile	7.7	67.2	25.5	7.3	5.5	5.3	90.1	9.9	0	87	62
4	Acetonitrile	3.5	67.2	25.5	7.3	2.7	2.1	92.3	7.7	0	72	55

m_{start}(CUR): calculated amount of CUR in the mixture of CURDs; m_{max}: max. achievable mass of CUR, based on the thermodynamic values; m(product): mass of the crystalline product gained; η_{TD}(CUR): max. thermodynamically possible yield of CUR; η(CUR): total product yield of CUR.
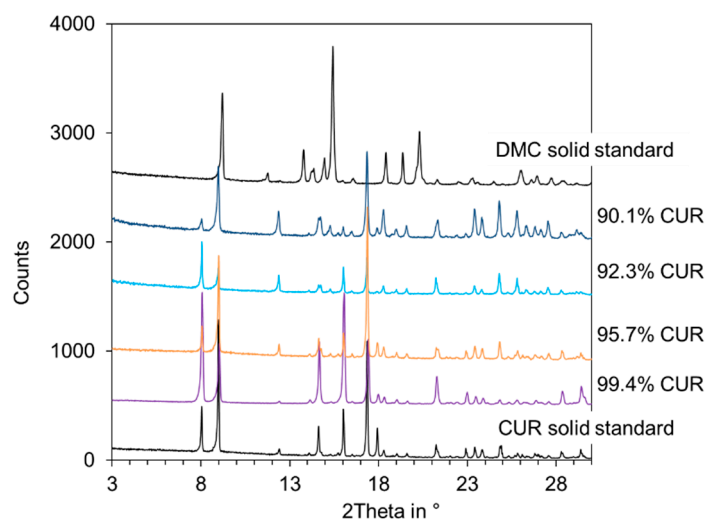

Figure 8. XRPD patterns of four crystallization products with increasing CUR content.

Since all XRPD reflexes in the diffractograms from the crystalline products can be clearly distinguished and are uniformly on the baseline, the presence of an amorphous fraction in the solid products cannot be confirmed. Moreover, all XRPD patterns seem to be identical to the CUR solid standard. Despite the increasing DMC content in the crystalline products (0.6–9.9%), none of the recorded patterns can be clearly assigned to the solid standard of DMC. Only a slight shift of single reflexes of crystalline products is indicated with increased DMC content in the solids.

Due to the strong similarity of CUR and DMC molecules, partial miscibility at the solid state might be a possible explanation here. However, dependent on the instrument and the structural similarity of the compounds used the limit of detection of the XRPD method is known to be 5–7 wt% and 1 wt%

in best cases. Thus, incorporation of DMC molecules is not readily assessable by XRPD at these low contents. Clarifying this issue requires further work which was out of the scope of this paper.

3.4. Improvement of the Total Yield by Means of Anti-Solvent Addition

To increase the product yield of the seeded cooling crystallization, it is suitable to conduct anti-solvent addition to the product suspension at the end of the cooling step [39]. In this work, to improve the overall yields of processes 1, 2 and 4 addition of water, 2-propanol and acetonitrile as anti-solvents of CUR in acetone was investigated. The final solvent/anti-solvent ratio was set to 25/75 (wt/wt). The study was conducted using the crude solid no. 1 with the lowest CUR content of 67.2%.

In the first step three equal starting solutions containing 8.5 wt% CUR in acetone were prepared and three identical seeded cooling crystallization processes were carried out as previously described in process no. 1. When the set end temperature of the cooling profile (0 °C) was reached, cold anti-solvent (< 0 °C) 2-propanol (process 1–2) and acetonitrile (process 1–3) was added to the product suspension, respectively (see Table 7). Afterwards the system was stirred for 3 h at constant 0 °C. The addition of water (process 1–1) was carried out at 26 °C after introducing CUR seeds to the supersaturated acetone solution. Then the suspension was cooled down to the end temperature 0 °C and stirred also for 3 h. Solid-liquid phase separation was performed at the end of each anti-solvent crystallization process. The crystalline products were dried at 40 °C and the CUR purity and yield analyzed. To maintain the total product yield and avoid the previously observed dissolution of the filter cake during washing with cold acetone, the washing step was skipped. The results obtained are summarized in Table 7.

Table 7. Overview of the results to improve total product yield (η(CUR)) via anti-solvent addition.

Process No.	Solvent	m_{start}(CUR)	CUR content	DMC content	BDMC content	m (product)	CUR content	DMC content	BDMC content	η (CUR)
		Ternary Mixture of Curcuminoids				**Crystalline Product**				
		g	%	%	%	g	%	%	%	%
1-1	25/75 acetone/water	2.9	**67.2**	25.5	7.3	2.7	**85.5**	13.4	1.1	**79**
1-2	25/75 acetone/2-propanol	2.9	**67.2**	25.5	7.3	1.1	**96.2**	3.7	0.1	**36**
1-3	25/75 acetone/acetonitrile	2.9	**67.2**	25.5	7.3	2.3	**88.3**	10.8	0.9	**70**

In all processes, addition of anti-solvent to the product suspension at the end of the cooling step led to a significant increase of yields. However, the CUR purity in the final crystalline products was noticeably decreased. DMC and in addition low amounts of BDMC (≤1.1%) were present as impurities. In addition to a detrimental effect of abstaining from product washing, an anti-solvent effect on DMC and BDMC cannot be excluded here (even solubility of DMC and BDMC is reported to exceed that of CUR in acetonitrile and isopropanol [34]). However, similar to the cooling crystallization (Table 6), the use of 2-propanol as anti-solvent (process 1–2) provided CUR at highest purity (96.2%) but at significantly lowest yield (36%). Regarding the reduced yield in presence of 2-propanol it can only be presumed at this stage, that, as indicated in polythermal (non-seeded) solubility studies from 2-propanol, an additional metastable (and thus higher soluble) polymorph or solvate phase occurs which causes the respective CUR remaining in the solution phase and thereby reducing the CUR yield in the solid phase.

4. Conclusions

In this work, the solubility behavior of pure CUR and CUR in presence of the two main impurities DMC and BDMC as well as supersolubilities in acetone, acetonitrile, methanol, ethanol, 2-propanol and their binary mixtures were investigated first. Based on the data obtained, seeded cooling crystallizations in four different process solvents (acetone, acetonitrile and 50/50 (wt/wt) mixtures of acetone/2-propanol and acetone/acetonitrile) were designed and implemented. As a result, the purity of CUR could be increased from initial CUR contents of 67–75% in the curcuminoid mixtures up to values of 90.1–99.4% in a single crystallization step. All crystallization processes provided crystalline curcumin (form I) free of BDMC after this single crystallization step. DMC was significantly depleted from initial contents of 19.2–25.5% in the crude mixtures to residual contents of 0.6–9.9%. Total product yields were significantly enhanced to 70–79% via addition of water and acetonitrile as anti-solvents at the end of the cooling crystallization process.

The presence of crystalline or amorphous DMC in the CUR products could not be detected by XRPD analysis. Whether this is caused by experimental detection limits or by potential formation of CUR/DMC mixed crystals has to be clarified in future studies.

Based on the work presented, a seeded cooling crystallization from a 50/50 (wt/wt) acetone/2-propanol solvent mixture is seen as the best purification strategy providing CUR at highest purity of 99.4%, BDMC free in a single crystallization step. However, there is still space for process optimization in particular with respect to yield. This includes application of a reduced cooling rate and a lowered final cooling temperature to increase both crystallization and total yield. Further, to avoid product losses in downstream processing washing the product with an acetone/anti-solvent mixture (for example acetonitrile) is suggested. No information regarding the maximum admissible limit of BDMC and DMC in the crystalline CUR was found in the literature. However, in any case the CUR purification grade obtained within a simple single crystallization step in this study represents a significant improvement compared to alternative process concepts.

References

1. Abdul, R.; Hatifah, P.L.; Ratna, W.; Muhammad, K. Use of Thin Layer Chromatography and FTIR Spectroscopy Along with Multivariate Calibration for Analysis of Individual Curcuminoid in Turmeric (*Curcuma longa* Linn) Powder. *Int. J. Pharm. Clin. Res.* **2016**, *8*, 419–424.
2. Bagchi, A. Extraction of Curcumin. *IOSR J. Environ. Sci. Toxicol. Food Technol.* **2012**, *1*, 1–16. [CrossRef]
3. Tanaka, K.; Kuba, Y.; Sasaki, T.; Hiwatashi, F.; Komatsu, K. Quantitation of curcuminoids in curcuma rhizome by near-infrared spectroscopic analysis. *J. Agric. Food Chem.* **2008**, *56*, 8787–8792. [CrossRef] [PubMed]
4. Priyadarsini, K.I. Chemical and structural features influencing the biological activity of curcumin. *Curr. Pharm. Des.* **2013**, *19*, 2093–2100. [PubMed]
5. Esatbeyoglu, T.; Hübbe, P.; Ernst, I.M.A.; Chin, D.; Wagner, A.E.; Rimbach, G. Curcumin From Molecule to Biological Function. *Angew. Chem. Int. Ed.* **2012**, *51*, 5308–5332. [CrossRef] [PubMed]
6. Patil, M.B.; Taralkar, S.V.; Sakpal, V.S.; Shewale, S.P.; Sakpal, R.S. Extraction, isolation, and evaluation of anti-inflammatory activity of curcuminoids from Curcuma longa. *Int. J. Chem. Sci. Appl.* **2011**, *2*, 172–174.

7. Esatbeyouglu, T.; Ulbrich, K.; Rehberg, C.; Rohn, S.; Rimbach, G. Thermal stability, antioxidant, and anti-inflammatory activity of curcumin and its degradation product 4-vinyl guaiacol. *Food Funct.* **2015**, *6*, 887–893. [CrossRef]

8. Yanagisawa, D.; Shirai, N.; Amatsubo, T.; Taguchi, H.; Hirao, K.; Urushitani, M.; Morikawa, S.; Inubushi, T.; Kato, M.; Kato, F.; et al. Relationship between the tautomeric structures of curcumin derivatives and their Abeta-binding activities in the context of therapies for Alzheimer's disease. *Biomaterials* **2010**, *31*, 4179–4185. [CrossRef]

9. Aggarwal, B.B.; Gupta, S.C.; Sung, B. Curcumin: An orally bioavailable blocker of TNF and other pro-inflammatory biomarkers. *J. Pharm.* **2013**, *169*, 1672–1692. [CrossRef]

10. Anand, P.; Sundaram, C.; Jhurani, S.; Kunnumakkara, A.B.; Aggarwal, B.B. Curcumin and cancer: An "old-age" disease with an "age-old" solution. *Cancer Lett.* **2008**, *267*, 133–164. [CrossRef]

11. Salem, M.; Rohani, S.; Gillies, E.R. Curcumin, a promising anti-cancer therapeutic: A review of its chemical properties, bioactivity and approaches to cancer cell delivery. *Rsc Adv.* **2014**, *4*, 10815. [CrossRef]

12. Chin, D.; Huebbe, P.; Pallauf, K.; Rimbach, G. Neuroprotective Properties of Curcumin in Alzheimer's Disease–Merits and Limitations. *Curr. Med. Chem.* **2013**, *20*, 3955–3985. [CrossRef]

13. Eckert, G.P.; Schiborr, C.; Hagl, S.; Abdel-Kader, R.; Muller, W.E.; Rimbach, G.; Frank, J. Curcumin prevents mitochondrial dysfunction in the brain of the senescence-accelerated mouse-prone 8. *Neurochem. Int.* **2013**, *62*, 595–602. [CrossRef]

14. Lee, W.H.; Loo, C.Y.; Bebawy, M.; Luk, F.; Mason, R.S.; Rohanizadeh, R. Curcumin and its Derivatives: Their Application in Neuropharmacology and Neuroscience in the 21st Century. *Curr. Neuropharmacol.* **2013**, *11*, 338–378. [CrossRef]

15. Johnson, J.J.; Mukhtar, H. Curcumin for chemoprevention of colon cancer. *Cancer Lett.* **2007**, *255*, 170–181. [CrossRef]

16. Simon, A. Inhibitory effect of curcuminoids on MCF-7 cell proliferation and structure-activity relationship. *Cancer Lett.* **1998**, *129*, 111–116. [CrossRef]

17. Ruby, A.J.; Kuttan, G.; Dinesch Badu, K.; Rajasekharan, K.N.; Kuttan, R. Anti-tumor and antioxidant activity of natural corcuminoids. *Cancer Lett.* **1995**, *94*, 79–83. [CrossRef]

18. Luis, P.B.; Boeglin, W.E.; Schneider, C. Thiol Reactivity of Curcumin and Its Oxidation Products. *Chem. Res. Toxicol.* **2018**, *31*, 269–276. [CrossRef]

19. Modasiya, M.K.; Patel, V.M. Studies on solubility of curcumin. *Int. J. Pharm. Life Sci.* **2012**, *3*, 1490–1497.

20. Carvalho, D.M.; Takeuchi, K.P.; Geraldine, R.M.; Moura, C.J.; Torres, M.C.L. Production, solubility and antioxidant activity of curcumin nanosuspension. *Food Sci. Technol.* **2015**, *35*, 115–119. [CrossRef]

21. Wanninger, S.; Lorenz, V.; Subhan, A.; Edelmann, F.T. Metal complexes of curcumin - synthetic strategies, structures and medicinal applications. *Chem. Soc. Rev.* **2015**, *44*, 4986–5002. [CrossRef] [PubMed]

22. Nandakumar, D.N.; Nagaraj, V.A.; Vathsala, P.G.; Rangarajan, P.; Padmanaban, G. Curcumin-artemisinin combination therapy for malaria. *Antimicrob. Agents Chemother.* **2006**, *50*, 1859–1860. [CrossRef] [PubMed]

23. Chaitanya Mannava, M.K.; Suresh, K.; Bommaka, M.K.; Konga, D.B.; Nangia, A. Curcumin-Artemisinin Coamorphous Solid: Xenograft Model Preclinical Study. *Pharmaceutics* **2018**, *10*, 7. [CrossRef] [PubMed]

24. Pabon, H.J.J. A synthesis of curcumin and related compounds. *Recl. Trav. Chim. Pays-Bas* **1964**, *83*, 379–386. [CrossRef]

25. Kim, E.J.; Cha, M.H.; Kim, B.-G.; Ahn, J.-H. Production of Curcuminoids in Engineered Escherichia coli. *J. Microbiol. Biotechnol.* **2017**, *27*, 975–982. [CrossRef] [PubMed]

26. Grynkiewicz, G.; Ślifirski, P. Curcumin and curcuminoids in quest for medicinal status. *Acta Biochim. Pol.* **2012**, *59*, 201–212. [CrossRef]

27. Pothitirat, W.; Gritsanapan, W. Quantitative analysis of curcumin, demethoxycurcumin and bisdemethoxycurcumin in the crude curcuminoid extract from Curcuma Longa L. in Thailand by TLC-Densitometry. *Mahidol Univ. J. Pharm. Sci.* **2005**, *32*, 23–30.

28. Aggarwal, B.B.; Bhatt, I.D.; Ichikawa, H.; Ahn, K.S.; Sethi, G.; Sandur, S.K.; Sundaram, C.; Seeram, N.; Shishodia, S. Curcumin-Biological and medicinal properties. In *Turmeric the Genus Curcuma*; Ravindran, P.N., Babu, K.N., Sivaraman, K., Eds.; CRC Press: Abingdon, UK, 2007; pp. 297–368.

29. Priyadarsini, K.I. The chemistry of curcumin: From extraction to therapeutic agent. *Molecules* **2014**, *19*, 20091–20112. [CrossRef]

30. Anderson, A.M.; Mitchell, M.S.; Mohan, R.S. Isolation of curcumin from turmeric. *J. Chem. Educ.* **2000**, *77*, 359–360. [CrossRef]

31. Revathy, S.; Elumalai, S.; Benny, M.; Antony, B. Isolation, Purification and Identification of Curcuminoids from Turmeric (*Curcuma longa* L.) by Column Chromatography. *J. Exp. Sci.* **2011**, *2*, 21–25.

32. Péret-Almeida, L.; Cherubino, A.P.F.; Alves, R.J.; Dufossé, L.; Glória, M.B.A. Separation and determination of the physico-chemical characteristics of curcumin, demethoxycurcumin and bisdemethoxycurcumin. *Food Res. Int.* **2005**, *38*, 1039–1044. [CrossRef]

33. Liu, J.; Svard, M.; Hippen, P.; Rasmuson, A.C. Solubility and crystal nucleation in organic solvents of two polymorphs of curcumin. *J. Pharm. Sci.* **2015**, *104*, 2183–2189. [CrossRef] [PubMed]

34. Ukrainczyk, M.; Hodnett, B.K.; Rasmuson, A.C. Process Parameters in the Purification of Curcumin by Cooling Crystallization. *Org. Process Res. Dev.* **2016**, *20*, 1593–1602. [CrossRef]

35. Horvath, Z.; Horosanskaia, E.; Lee, J.W.; Lorenz, H.; Gilmore, K.; Seeberger, P.H.; Seidel-Morgenstern, A. Recovery of Artemisinin from a Complex Reaction Mixture Using Continuous Chromatography and Crystallization. *Org. Process Res. Dev.* **2015**, *19*, 624–634. [CrossRef]

36. Heffernan, C.; Ukrainczyk, M.; Gamidi, R.K.; Hodnett, B.K.; Rasmuson, A.C. Extraction and Purification of Curcuminoids from Crude Curcumin by a Combination of Crystallization and Chromatography. *Org. Process Res. Dev.* **2017**, *21*, 821–826. [CrossRef]

37. Horosanskaia, E.; Triemer, S.; Seidel-Morgenstern, A.; Lorenz, H. Purification of Artemisinin from the Product Solution of a Semisynthetic Reaction within a Single Crystallization Step. *Org. Process Res. Dev.* **2019**, *23*, 2074–2079. [CrossRef]

38. Horosanskaia, E.; Nguyen, T.M.; Vu, T.D.; Seidel-Morgenstern, A.; Lorenz, H. Crystallization-Based Isolation of Pure Rutin from Herbal Extract of Sophora japonica L. *Org. Process Res. Dev.* **2017**, *21*, 1769–1778. [CrossRef]

39. Wiekhusen, D. Development of batch crystallizations. In *Crystallization—Basic Concepts and Industrial Applications*; Beckmann, W., Ed.; Wiley-VCH Verlag GmbH & Co. KGaA: Weinheim, Germany, 2013; pp. 187–202.

40. Jadhav, B.K.; Mahadik, K.R.; Paradkar, A.R. Development and validation of improved reversed phase HPLC method for simultaneous determination of curcumin, demethoxycurcumin and bis-demethoxycurcumin. *Chromatographia* **2007**, *65*, 483–488. [CrossRef]

41. Lorenz, H. Solubility and solution equilibria in crystallization. In *Crystallization – Basic Concepts and Industrial Applications*; Beckmann, W., Ed.; Wiley-VCH Verlag GmbH & Co. KGaA: Weinheim, Germany, 2013; pp. 35–74.

42. Sanphui, P.; Goud, N.R.; Khandavilli, U.B.; Bhanoth, S.; Nangia, A. New polymorphs of curcumin. *Chem. Commun.* **2011**, *47*, 5013–5015. [CrossRef]

43. Gately, S.; Triezenberg, S.J. Solid Forms of Curcumin. U.S. Patent WO2012138907A2, 20 September 2012.

44. Mishra, M.K.; Sanphui, P.; Ramamurty, U.; Desiraju, G.R. Solubility-Hardness Correlation in Molecular Crystals: Curcumin and Sulfathiazole Polymorphs. *Cryst. Growth Des.* **2014**, *14*, 3054–3061. [CrossRef]

45. Thorat, A.A.; Dalvi, S.V. Solid-State Phase Transformations and Storage Stability of Curcumin Polymorphs. *Cryst. Growth Des.* **2015**, *15*, 1757–1770. [CrossRef]

46. Tonnesen, H.H.; Karlsen, J.; Mostad, A. Structural Studies of Curcuminoids. I. The Crystal Structure of Curcumin. *Acta Chem. Scand.* **1982**, *36*, 475–479. [CrossRef]

47. Tonnesen, H.H.; Karlsen, J.; Mostad, A.; Pedersen, U.; Rasmussen, P.B.; Lawesson, S.-O. Structural Studies of Curcuminoids. II. Crystal Structure of 1,7-Bis(4-hydroxyphenyl)-1,6-heptadiene-3,5-dione-Methanol Complex. *Acta Chem. Scand.* **1983**, *37*, 179–185. [CrossRef]

48. Karlsen, J.; Mostad, A.; Tonnesen, H.H. Structural studies of curcuminoids. VI. Crystal structure of 1,7_bis(4-hydroxyphenyl)-1,6-heptadiene-3,5-dione hydrate. *Acta Chem. Scand.* **1988**, *42*, 23–27. [CrossRef]

49. Yuan, L.; Horosanskaia, E.; Engelhardt, F.; Edelmann, F.T.; Couvrat, N.; Sanselme, M.; Cartigny, Y.; Coquerel, G.; Seidel-Morgenstern, A.; Lorenz, H. Solvate formation of bis(demethoxy)curcumin: Crystal structure analyses and stability investigations. *Cryst. Growth Des.* **2019**, *19*, 854–867. [CrossRef]

50. Yuan, L.; Lorenz, H. Solvate formation of bis(demethoxy)curcumin: Screening and characterization. *Crystals* **2018**, *8*, 407. [CrossRef]